Clin Transl Imaging (2014) 2:391–401
DOI 10.1007/s40336-014-0084-9

REVIEW ARTICLE

Multimodality molecular imaging of the lung

Delphine L. Chen · Paul E. Kinahan

Received: 24 August 2014 / Accepted: 29 September 2014 / Published online: 16 October 2014

Abstract Lung diseases cause significant morbidity and mortality and lead to high healthcare utilization. However, few lung disease-specific biomarkers are available to accurately monitor disease activity for the purposes of clinical management or drug development. Advances in cross-modal imaging technologies, such as combined positron emission tomography (PET) and magnetic resonance (MR) imaging scanners and PET or single-photon emission computed tomography (SPECT) combined with computed tomography (CT), may aid in the development of noninvasive, molecular-based biomarkers for lung disease. However, the lungs pose particular challenges in obtaining accurate quantification of imaging data due to the low density of the organ and breathing motion. This review covers the basic physics underlying PET, SPECT, CT, and MR lung imaging and presents technical considerations for multimodal imaging with regard to PET and SPECT quantification. It also includes a brief review of the current and potential clinical applications for these hybrid imaging technologies.

Keywords Molecular imaging · Multimodality imaging · Lung disease · Lung cancer · Positron emission tomography · Single photon emission computed tomography · Magnetic resonance imaging

Color figures online at http://link.springer.com/article/10.1007/s40336-014-0084-9

D. L. Chen
Department of Internal Medicine, Washington University School of Medicine, St. Louis, MO, USA

D. L. Chen (✉)
Division of Radiological Sciences and Nuclear Medicine, Mallinckrodt Institute of Radiology, Campus Box 8225, 510 S. Kingshighway Blvd, St. Louis, MO 63110, USA
e-mail: chend@mir.wustl.edu

P. E. Kinahan
Department of Radiology and Bioengineering and Physics, University of Washington Medical Center, Seattle, WA, USA

Introduction

Chronic lung disease leads to the second highest utilization of inpatient hospital care behind cardiovascular disease and is the third leading cause of mortality behind cardiovascular and oncologic disease in the United States [1]. Worldwide, chronic obstructive pulmonary disease (COPD) alone is projected to be the fourth leading cause of death by 2030 [2] with asthma also contributing significantly to the overall lung disease burden [1]. Furthermore, lung cancer is the leading cause of cancer deaths in the United States and has one of the lowest five-year survival rates after diagnosis, higher only than those of pancreatic and liver cancer [3]. Despite this significant disease burden, few therapeutics have been developed that significantly alter the natural course of these diseases.

The lack of effective therapeutics has been attributed in part to the inadequacy of available specific biomarkers for lung disease activity [4]. For non-oncologic disease, pulmonary function testing (PFT) continues to be a mainstay of clinical lung function assessment; however, PFT does not provide any specific information about the underlying process causing lung function loss in a given lung disease. Gold standard tests for lung inflammation such as bronchoalveolar lavage (BAL) also contribute important information regarding cell recruitment in the airways; however, information regarding the activity of these cells can be challenging to assess by BAL alone. Given that many lung diseases affect the lung heterogeneously both spatially and

temporally, sampling limitations can compromise the accuracy of tissue-based assays for characterizing disease activity across the entire lungs. In oncologic disease, the mechanisms underlying disease progression and treatment resistance also remain unclear. Therefore, the development of new biomarkers that can provide both global and regional disease-specific measurements has the potential to improve our understanding of the underlying causes of these diseases. Such biomarkers could also aid in the translation of novel therapeutics by confirming mechanisms of action in vivo or demonstrating earlier evidence of benefit.

Molecular imaging has the potential to contribute important information regarding both oncologic and non-oncologic disease activity that is not easily obtained by available methods. Modalities such as positron emission tomography (PET) and single-photon emission computed tomography (SPECT) enable the noninvasive, quantitative assessment of the whole lungs, thus allowing both global and regional assessments of disease activity. Because the radiolabeled tracers used to generate these images can target nearly any cellular pathway or receptor with the injection of very low mass amounts, more specific information regarding cell trafficking and activity can be obtained more readily by these than by other modalities. The addition of computed tomography (CT) and/or magnetic resonance (MR) imaging also allows the combination of anatomical, functional and additional molecular information to better characterize lung disease.

In this review, we discuss the technical challenges facing imaging systems for providing quantitative molecular biomarkers of lung disease activity. With regard to CT and MR imaging specifically, there have been substantial developments in advanced imaging methods and applications. A thorough review of these developments is beyond the scope of this review, although we do mention these where they have an impact on multimodal imaging. We consider PET and SPECT image processing in the light of the PET/MR systems now available, opportunities for new tracers and clinical applications, and the clinical potential of combining information from PET/CT, PET/MR, and SPECT/CT for assessing lung disease.

Comparing molecular imaging modalities

Imaging physics

PET

The fundamental role of a PET scanner is to form an image of the spatially varying concentration of targeted tracers labeled with a positron emitter [5]. PET tracers comprise a positron emitter attached to a biological substrate or a drug targeting a cellular pathway or receptor of interest. For example, ^{18}F-fluorodeoxyglucose (^{18}F-FDG), which is used for $\sim$90 % of all clinical PET imaging studies, comprises an F-18 atom replacing the hydroxyl group on the 2-carbon position of glucose. With corrections for physical effects, most notably attenuation as well as scatter, accurate estimates of the direct concentration of PET tracers within various tissues can be obtained. To account for variations in the injected dose and patient size, the generally preferred unit for clinical use is the standardized uptake value (SUV) defined as $\mathrm{SUV} = R/\left(d'/\tilde{V}\right)$ [6, 7], where R (kBq/ml) is the activity concentration within a region of interest (ROI), d' (kBq) is the decay-corrected injected dose, and $\tilde{V}$ is a surrogate for the volume of tracer distribution in the body. Typically, patient weight (kg) is used as a surrogate for the volume of distribution, in which case SUV units are g/ml. Since adipose tissue, with the exception of brown fat, does not normally take up significant amounts of ^{18}F-FDG, the estimated lean body mass or body surface area is sometimes used instead of weight. Unique advantages of PET include its very high sensitivity (typically detecting $\sim$5 % of all radioactive decays), and its quantitative accuracy with proper calibration [8, 9].

SPECT

Like PET, SPECT also provides tomographic images of radiolabeled tracers using single-photon counting [5]. Detecting only single photons, however, leads to a relative disadvantage of three orders of magnitude in the resolution/sensitivity trade-off when compared to PET. As practiced in clinical imaging, SPECT typically has lower resolution and significantly lower sensitivity than PET. However, higher resolution than PET is possible at the expense of even lower sensitivity, although this requires either longer imaging times or restricted imaging areas. The quantitative accuracy of regional tracer measurements with SPECT is more challenging than with PET due to depth-dependent attenuation and collimator blurring, which cannot easily be corrected from the SPECT images alone due to the physics of single-photon detection [5]. However, with the wider availability of SPECT/CT scanners, the CT images can now be used to create an attenuation map for the SPECT data. The potential for improved quantitation and anatomical localization (similar to what can be obtained with PET/CT scanners) has led to renewed interest in improving SPECT quantitation and in new clinical applications, as discussed below.

CT and MR for lung imaging

Imaging the lung with CT uses X-ray photons and provides an accurate image of tissue density differences; thus, CT is an established, clinically useful modality for imaging the

lungs as it provides exquisite detail of the lung parenchyma architecture. In CT lung imaging, an adult patient incurs an effective radiation dose of approximately 5–8 mSv [12]. However, given the extensive use of chest CT for thoracic evaluation, research efforts have focused on various algorithms to reduce the radiation dose while maintaining acceptable image quality [13–15]. In cystic fibrosis patients, iterative reconstruction techniques can lower the radiation dose levels significantly, achieving effective doses of 0.04–0.05 mSv per chest CT, without significantly sacrificing image quality. This approach works particularly well for conditions with a significant soft tissue component such as bronchiectasis and abscesses [16]. Novel image reconstruction approaches may help to further reduce the radiation exposure associated with chest CT exams without compromising the evaluation of the lung parenchyma [15]. Such advances will help to minimize the potential radiation risks for patients with lung disease who frequently require repeated CT or other radiographic measurements. Importantly, these radiation exposures should be compared to the typical effective dose per year from naturally occurring sources (i.e., background radiation levels), which has a range of approximately 1–10 mSv, depending on where one lives. The American Association of Physicists in Medicine has stated that "Risks of medical imaging at effective doses below 50 mSv for single procedures or 100 mSv for multiple procedures over short time periods are too low to be detectable and may be nonexistent." [17]. Thus, improvements in managing CT-related radiation doses will help minimize related risks for patients with lung disease. In relation to multimodal imaging, the typical trend in technology and application advancement is that new features in CT (or MR imaging) will often migrate to the respective modality on a multimodality scanner. Indeed, the low dose and iterative reconstruction strategies described above for CT are already gradually being introduced into PET/CT and SPECT/CT scanners. It is not clear whether the different approaches for advanced CT techniques, such as dual-energy CT, will be incorporated into PET/CT and SPECT/CT scanners. However, the development of clinical or research applications in which simultaneous acquisition of this information with PET or SPECT is essential will likely drive the adoption of these more advanced CT techniques on PET/CT or SPECT/CT scanners.

MR imaging in the lung, on the other hand, presents two well-known challenges: lack of signal as a result of the relatively low concentration of hydrogen nuclei due to low tissue density, and distortions arising from sharp gradients of the magnetic susceptibility at the tissue/air interfaces. Many of these problems can be overcome using a rapid, spin echo-based imaging sequence that utilizes respiratory and/or cardiac gating and minimizes the signal from other tissue [10, 11]. These approaches are especially attractive now that PET/MR scanners are commercially available, opening the possibility of merging anatomical information in addition to the other unique information provided by MR with PET. Hyperpolarized helium imaging is one example in which an inhaled contrast agent increases the signal in the lungs to enable detailed structural analyses. Such approaches are now used extensively for research purposes. While it is not clear whether PET/MR scanners will have the capability for hyperpolarized helium MR or other advanced MR imaging methods, the addition of such capabilities would improve the ability to directly correlate functional MR measures with molecular information obtained by PET.

Quantification approaches

PET

One of the primary advantages of PET is the ease with which tracer accumulation in a tissue or ROI can be quantified. Both static and dynamic (i.e., time-varying) measurements can be obtained with PET. Static measurements, such as the SUV, are based on the number of counts measured at a particular time point within a given ROI. The SUV is easily calculated and frequently used in clinical practice. By contrast, measurements from dynamic imaging procedures are more complex but allow more sophisticated calculations of tracer uptake, such as rates of tracer movement or receptor-binding potential in a tissue of interest. Individual rate constants that define the movement of the tracer between different functional compartments within a tissue (e.g., transport of a tracer from the intravascular to extravascular space) can also be calculated. While static measurements are easy to obtain, they may not be as sensitive as rate measurements to small changes in tracer activity when overall uptake is low, such as in the lungs [18]. Therefore, dynamically acquired imaging data under these conditions may be better suited for quantifying tracers with low levels of uptake in lung parenchymal disease.

Uncertainty in PET measurements is known to be due to variations in the many steps in the imaging chain [19]. Dominant sources of error include differences in scanner capabilities, scanner calibration errors, differences in tracer uptake time, variations in quantitative corrections and reconstruction parameters as well as in analysis methods and tools, inherent biological differences between patients, and operator error. In comparing PET/CT versus PET/MR scanners, the two major differences are the changes in detector technology and the method estimating intrinsic attenuation of the 511 keV photons by patient tissue. The high magnetic fields within MR imaging scanners require

different PET detector technologies that can operate effectively within the magnetic field while not interfering with the MR scanner's image acquisition [20]. These technical requirements thus constrain the performance/cost ratio in terms of resolution, sensitivity and/or imaging field of view versus scanner cost. It is worth noting, however, that the detector technology improvements developed for PET/MR imaging may migrate to PET/CT scanners.

Quantitative PET imaging requires accurate attenuation correction. Estimating the attenuation of 511 keV photons from the PET tracer is straightforward with PET/CT but less so with PET/MR, as described below. The estimated attenuation factors are used for both attenuation and scatter correction, two of the dominant corrections in PET imaging. In addition, for the overall calibration of PET/CT scanners, it is possible to use NIST-traceable standards for absolute calibration [21]; however, for PET/MR, equivalent calibration standards do not yet exist. Thus, while well-accepted standards can validate the quantitative accuracy of PET/CT scanners (e.g., the ACR and NEMA PET standards), no consensus approach yet exists for validating the quantitative accuracy of PET/MR scanners. Nevertheless, it seems likely that such standards will emerge for PET/MR, given the increasing utilization of PET/MR for research and clinical applications [22].

SPECT

Both static and dynamic SPECT imaging data can be acquired to determine the level of tracer uptake in any given tissue. Attenuation correction is particularly important for SPECT quantification as the attenuation of the lower energy photons emitted by the radioisotopes used for SPECT imaging is significantly higher than that of the higher energy photons from PET radioisotopes. With the growing prevalence of SPECT/CT, attenuation correction can now be achieved more readily using the CT-based attenuation map, thus enabling quantitative SPECT to be used more regularly on a clinical basis. Imaging external radiotracer sources can also be used to improve the accuracy of these corrections for SPECT imaging and potentially to allow absolute measurements of tracer accumulation, as is inherently possible with PET imaging. The most common type of SPECT/CT scanner uses slowly rotating detector heads [23], which poses a challenge for dynamic imaging of rapidly varying tracer uptake. However, accurate parameter estimation in dynamic SPECT imaging is possible if certain constraints are met [24]. Once the accuracy of the SPECT data obtained is verified, the same kinetic modeling approaches used for PET can also be used for SPECT data. The count density is often an issue for SPECT compared with PET in the lungs, thus presenting particular challenges for accurately quantifying low levels of tracer uptake for parenchymal disease imaging.

Technical developments for multimodal imaging

Attenuation correction

Attenuation of the high-energy photons by patient tissue is a dominant physical effect in PET and SPECT imaging. For PET/CT and SPECT/CT imaging, the attenuation factors can be conveniently derived from the CT image as the same processes affect photon scattering in PET, SPECT and CT [25–27]. For MR imaging, however, the image values typically represent a weighted average of hydrogen proton density and T1 and T2 relaxation times, which are influenced by the local environment [28]. For qualitative PET/MR, current reconstruction algorithms using Dixon-based attenuation corrections yield comparable, and even slightly superior, PET images as evidenced by the improved resolution of the vertebral bodies on the PET images obtained on a Siemens mMR scanner (Fig. 1). However, accurate PET quantification depends on appropriate attenuation correction. MR image values (unlike CT image ones) do not directly reflect the tissue attenuation values, as illustrated by the comparison of the CT with the T2-HASTE MR whole-body images in Fig. 1. Thus, this inaccuracy in the MRI data can confound accurate PET or SPECT quantification. Of particular note is that the MR signal in bone is significantly different from the signal on the CT image. Greater differences in the blood and adipose tissue values are also apparent. Therefore, there is no simple scaling method that can be used to convert the MR image to a CT-equivalent attenuation map. Differences between CT and MR imaging information for lung parenchyma are further illustrated in Fig. 2, which compares CT and T2-weighted MR lung images, illustrating the lower MR intensity values in the lung due to the low density of hydrogen nuclei and possibly also due to susceptibility artifacts from the air–surface interfaces [29].

The current approach for attenuation correction, which circumvents the different physics in PET and MR imaging, is image segmentation to discriminate between air, lungs, fat and soft tissue, and the use of connected component analysis to identify the lungs, although bone is treated as soft tissue (Fig. 3). While this approach can lead to errors in the estimation of PET tracer uptake in bone, it is currently the most robust method for estimating PET tracer uptake in the lung from PET/MR data [30].

Respiratory motion correction

Accommodating respiratory motion to ensure that quantitative measures of lung tracer uptake are accurate is also a challenge, particularly with the development of PET/CT scanners. Because of the greater spatial and temporal resolution possible with CT scans, there is now a greater

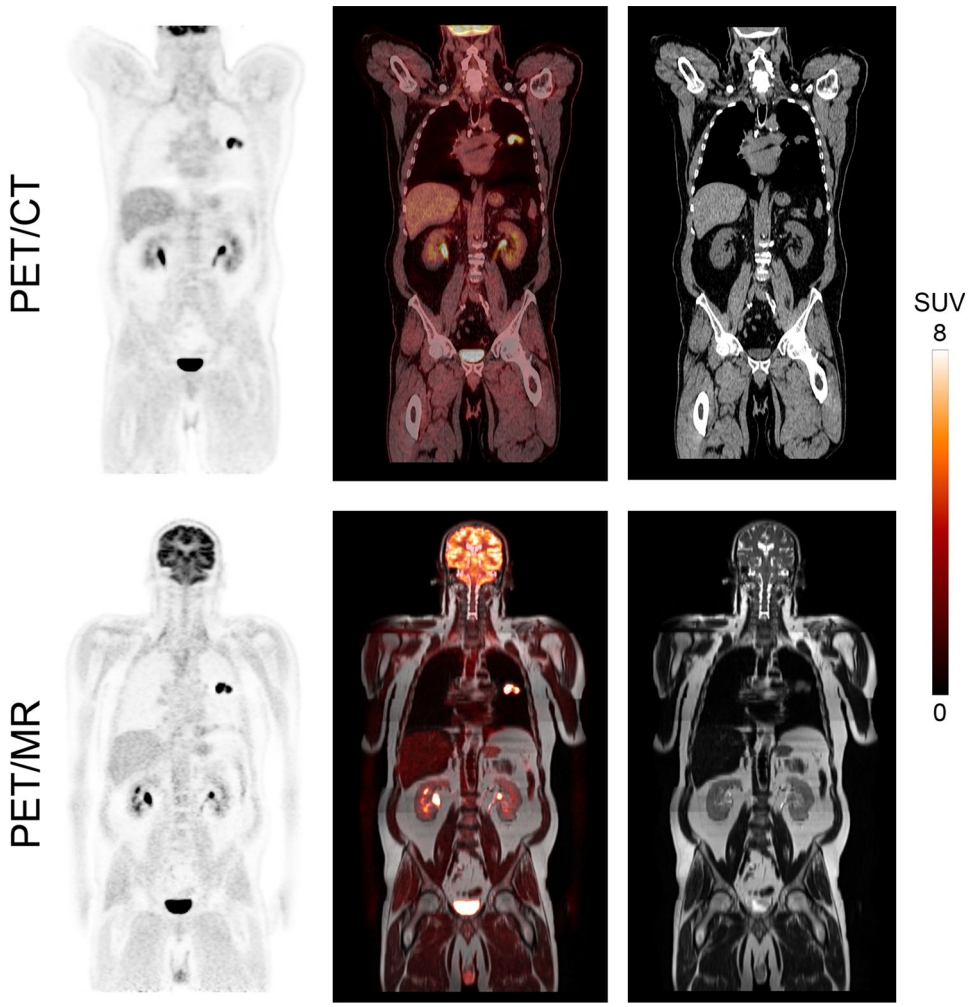

Fig. 1 PET/CT vs PET/MR images in a patient imaged by PET/CT at approximately 1 h after injection of 15 mCi of ^{18}F-FDG followed by PET/MR imaging at 1 h and 10 min after PET/CT imaging. Note that the PET images from the PET/MR scanner demonstrate better resolution of the vertebrae compared to the PET/CT images. In comparing the CT and MRI images, the bones on the MRI are similar in signal intensity to the fat due to the fat in the marrow, thus limiting the accuracy of using MRI-based values for generating an appropriate attenuation correction map. The tumor appears brighter on the PET/MR images because of the longer delay in imaging after tracer injection as the scans were performed serially on the same day in the same patient. Images courtesy of Akash Sharma and Jonathan McConathy, Mallinckrodt Institute of Radiology, Washington University School of Medicine, St. Louis, MO (color figure online)

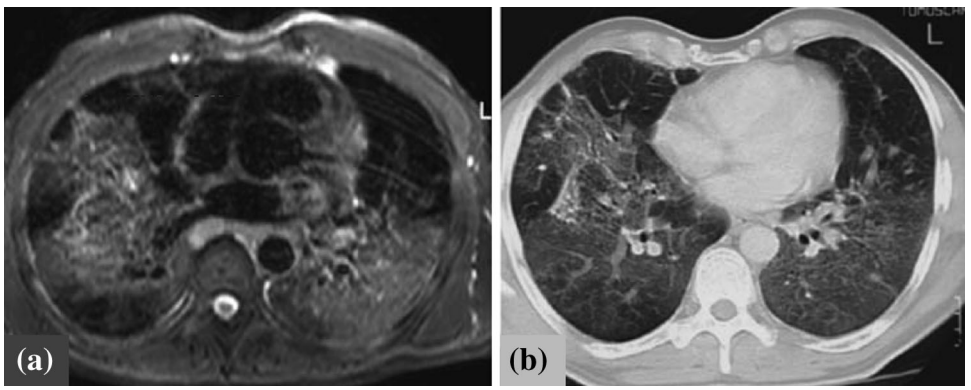

Fig. 2 T2-weighted MRI (**a**) and (**b**) CT images of the thorax of the same patient showing the lack of similarity of the physical properties measured [29]. (With kind permission from Springer Science + Business Media)

likelihood of attenuation correction artifacts and potential uncertainty when using the CT images for ROI placement. A variety of breathing protocols have been tested for clinical PET/CT imaging, with quiet free breathing or breath-holds at normal (in contrast to maximal) end-expiration demonstrated to be most useful for minimizing respiratory artifacts [31, 32]. There are, however, errors introduced by this approach [33, 34], and so several methods to compensate for respiratory motion have been proposed.

Respiratory motion compensation is important in quantitative multimodality molecular imaging of the lung. In the context of PET/CT imaging of the lung, considerable efforts have been made to develop appropriate methods for

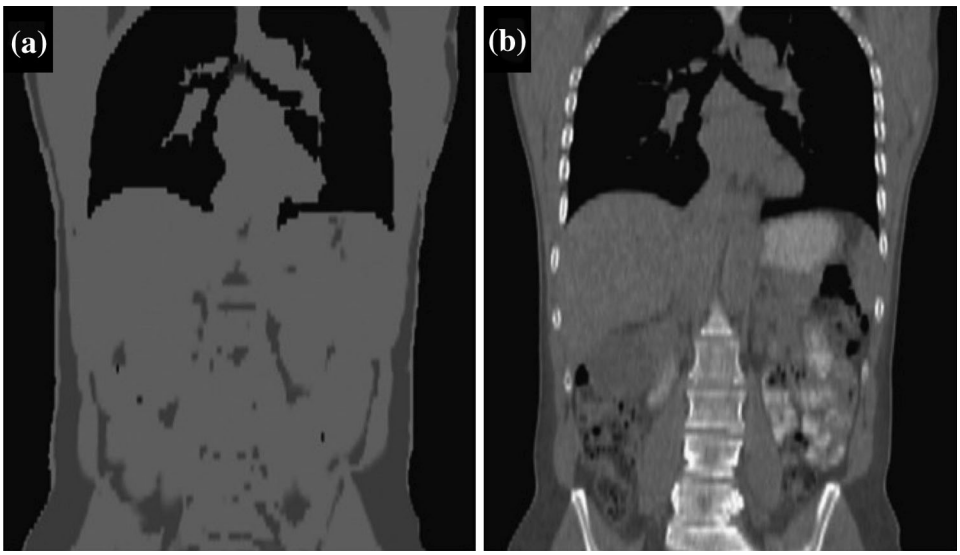

Fig. 3 **a** PET attenuation image formed by segmentation of MRI images. **b** CT-based attenuation map of same patient. This research was originally published in [30]. ©By the Society of Nuclear Medicine and Molecular Imaging, Inc

Table 1 Diagnostic accuracy of PET, CT and PET/CT

Tumor entity	References	Purpose of the imaging studies	Number of patients	Accuracy (%)		
				PET/CT	PET	CT
Head and neck	Chen et al. [35]	TNM staging	70	95	83[a]	73[a]
	Schoder et al. [36]	Lesion detection	68	96	90[a]	ND
NSCLC	Lardinois et al. [24]	T stage	40	98	80[a]	78[a]
		N stage	37	84	87	64
	Shim et al. [37]	T stage	106	86	ND	79
		N stage	106	84	ND	69[a]
Colorectal	Kim et al. [10]	Recurrence	51	88	71[a]	ND
	Votrubova et al. [38]	Recurrence	84	90	75[a]	ND
Lymphoma	Allen-Auerbach et al. [33]	(Re)staging	73	93	84[a]	ND
	la Fougère et al. [39]	(Re)staging	50	99	98	89[a]
Melanoma	Reinhardt et al. [31]	(Re)staging	250	97	93[a]	79[a]
	Mottaghy et al. [40]	(Re)staging	102	91	92	ND

Reprinted by permission from Macmillan Publishers LTD: [Nat Clin Pract Oncol], reference 42, copyright 2008

NSCLC non-small-cell lung cancer, *ND* not determined, *TMM* tumor node metastasis

[a] Statistically significant difference when compared with PET/CT

this (Table 1). The most direct approach is the use of respiratory gating to reduce the effects of respiratory motion blurring [35]. To compensate for inter-modality positional mismatch, one approach is to use time-averaged CT images [36] to approximately match the respiratory blurring that occurs during the PET image acquisition; however, this method is at best an approximate solution, and it also requires longer CT acquisition times, increasing the radiation dose delivered to the patient. A different approach is to use phase-matched respiratory-gated CT and PET images to jointly solve both respiratory motion blurring and inter-modality mismatch [37]. One of the difficulties with this approach, however, is the multitude of noisy images that are produced. This has led to the development of more sophisticated methods that remove respiratory motion artifacts of both types while preserving quantitative accuracy and without increasing noise [38].

These methods can be considered to some extent as a hierarchy, with more sophisticated (and complex) methods providing more accurate compensation for respiratory blurring and PET/CT mismatch. This is a rapidly advancing field, and a review of potential methods is beyond the scope of this report. A summary of these methods is given in Table 1, and a general overview is given in the review by Nehmeh and Erdi [39].

In PET/MR imaging of the lung, additional considerations apply. With the availability of clinical PET/MR systems, novel MR sequences are now being developed to measure respiratory motion during the PET imaging, thus enabling the application of advanced motion compensation

methods. It is possible, for example, to use MR navigator data to measure the location of the diaphragm during a PET scan. Respiration-gated PET data can then be co-registered using MR-derived motion fields to obtain a single motion-corrected PET image [40]. These early feasibility studies indicate that unique improvements in PET activity localization and quantification in the lung may be a feature of simultaneous PET/MR imaging.

Clinical applications

PET/CT and PET/MR

Cancer: diagnosis

PET/CT is now a standard approach for the diagnosis and staging of lung cancer [41]. PET clearly adds information that is not available from CT, thus improving the assessment of the primary tumor and of nodal and distant metastases [42]. Following the introduction of clinical PET/MR scanners, early work has focused on comparing the diagnostic value of PET/MR vs PET/CT imaging. Published studies of PET/MR imaging demonstrate that the PET image data are comparable to those obtained from PET/CT scanners [43–47]. However, the equivalence of SUV quantification from PET/MR scans has been found to be variable [48], with the potential reasons for this discussed previously in "Technical developments for multimodal imaging". The immediate value of PET/MR imaging in oncology, not surprisingly, appears to come from the improved diagnostic information regarding soft tissue lesions coming from the MR images [45, 46]. The benefit of whole-body PET/CT for detecting distant metastases in lung cancer and the potential added value of whole-body MR imaging has already been demonstrated in studies combining information from separate MR imaging and PET/CT acquisitions [49–51]. These studies together provide a rationale for investigating PET/MR as a diagnostic tool for improving whole-body assessments for lung cancer metastases.

With regard to staging nodal stations, it is still unclear whether PET/MR, when limited to the chest, contributes significantly different information from that provided by PET/CT [46, 52]. However, MR imaging information may be useful for further assessing the extent of primary tumor invasion by differentiating tumor from areas of consolidation [53]. This information could also be combined with metabolic information obtained using ^{18}F-FDG, for example, to better delineate the primary tumor. The use of novel PET tracers will likely further improve the diagnosis of lung cancers and help guide treatment choices to improve outcomes [54]. [^{18}F]fluorine-labeled thymidine and ^{18}F-FDG have been investigated for their prognostic value in predicting responses to erlotinib, a tyrosine kinase inhibitor [55–57]. New PET tracers like [^{11}C]choline have also been used with PET/MR for improved prostate cancer diagnosis [45]. In addition, the molecular information obtained by PET, as well as specific CT characteristics, may indicate the underlying genotype of a cancer [58, 59]. Thus, the combination of the unique information provided by each of these imaging approaches could be used not only to provide important diagnostic and prognostic information, but also to better stratify patients for targeted therapies.

Cancer: treatment planning

PET and CT are mainstays of radiotherapy treatment planning. Because the attenuation characteristics of CT X-rays best match those of the X-rays used for radiotherapy, CT is the gold standard for dosimetry determinations. However, the addition of PET for gross tumor volume delineation has improved the ability of radiotherapy to treat the biologically relevant tissues for effective tumor control. The chest presents special challenges given that respiratory motion can significantly reduce the accuracy of radiation dose delivery. Also, controlling the dose delivery in the lungs is particularly important to reduce the risk of developing radiation pneumonitis [60]. Thus, with the advent of PET/MR, it may be possible to leverage the motion-tracking capabilities of MR to improve PET target delineation. In addition, several retrospective studies have assessed the value of using ^{18}F-FDG PET to predict the risk of developing radiation pneumonitis [61–63], suggesting that prospective trials assessing ^{18}F-FDG PET in this role may be warranted. Thus, PET/MR may also have a role in identifying patients at risk of developing radiation pneumonitis. Further clinical studies will be needed to confirm the results of these retrospective studies.

COPD and cystic fibrosis

CT imaging is a mainstay of COPD and cystic fibrosis evaluation. The additional information provided by PET/MR promises to significantly advance our understanding of these chronic lung diseases. Both of these conditions are characterized by abnormally persistent lung inflammation that presumably leads to lung tissue destruction [64, 65]. However, despite the known presence of inflammation in these diseases, most clinical decisions are still based on PFT without the benefit of specific inflammatory measures. The development of appropriate lung inflammation biomarkers may thus provide new information that could be used clinically to guide therapy decisions, particularly for targeted anti-inflammatory therapies.

To date, only a small number of subjects with either COPD or cystic fibrosis have been evaluated with ^{18}F-FDG PET, but the available data suggest that ^{18}F-FDG PET can in fact quantify lung inflammation levels and may thus be a useful biomarker of inflammatory cell activity. In COPD, two published studies have demonstrated increased ^{18}F-FDG uptake in affected patients, presumably due to increased inflammation [66, 67]. Both these studies used the Patlak graphical analysis to quantify ^{18}F-FDG uptake. A third study demonstrated that differences in ^{18}F-FDG uptake could also be determined using the CT scan to normalize SUV measurements for density [68]. In cystic fibrosis, ^{18}F-FDG uptake is also increased in the lungs and does not always correlate to underlying CT abnormalities [69]. ^{18}F-FDG uptake may also serve as a biomarker for treatment response as antibiotic therapy rapidly reduces ^{18}F-FDG uptake in patients with acute exacerbations [69, 70]. However, the numbers of patients studied remain small; larger studies will be needed to further confirm the potential clinical utility of ^{18}F-FDG PET in these patient populations. In addition, the quantification approach for summarizing PET data in these diseases remains to be determined. Therefore, the technical aspects of ensuring accurate, quantitative PET data from both PET/CT and PET/MR scanners will be critical in ensuring the development of robust PET measures of these lung diseases.

MR imaging with hyperpolarized ^{3}He has also shown promise for assessing alveolar structure and function in COPD and cystic fibrosis. Ventilation defects visualized by hyperpolarized 3He also resolve after antibiotic therapy in cystic fibrosis patients with acute exacerbation, indicating the potential for imaging the functional consequences of such treatments [71]. ^{3}He MR imaging may also predict those COPD patients at risk of acute exacerbations [72]. The availability of PET/MR scanners thus creates opportunities for studying the relationship of glucose utilization rates or uptake of novel PET tracers (as more specific markers of inflammation) with regional lung function in these diseases. Unfortunately, the currently available PET/MR scanners lack the multinuclear packages needed to acquire images with hyperpolarized gas or other novel MR contrast agents, thus limiting the MR assessment of the lungs in such diseases. Nevertheless, current PET/MR scanners allow PET information to be integrated with information from proton-based or post-contrast lung images. Improvements in ultra-fast echo sequences that can visualize the lung parenchyma also promise to allow lung parenchymal assessment without the ionizing radiation of CT [10, 11], thus potentially opening the way for PET/CT like assessments with reduced radiation exposure. In addition, if multinuclear packages can be incorporated into PET/MR scanner software, PET/MR scanners will have the unique feature of being able to simultaneously acquire novel information regarding multiple facets of lung cellular activity, structure and function and thereby to help investigators determine the relationships between these different levels of lung function [73]. The ability to acquire both PET and MR data simultaneously will also improve the efficiency by which these data can be obtained. The clinical utility of these approaches remains to be determined.

SPECT and SPECT/CT

Ventilation and perfusion assessment

SPECT and SPECT/CT for ventilation and perfusion scintigraphy has recently been reviewed in detail (see issue for reference 74). As a result of improved contrast and 3D representation of imaging data with SPECT, improved sensitivity for detecting ventilation and perfusion defects can be achieved with current SPECT and SPECT/CT systems [74]. With the growing availability of SPECT/CT scanners, combined ventilation and perfusion imaging may also improve the diagnostic specificity by incorporating the CT image data into the ventilation/perfusion defect assessment. Quantitative SPECT is also more easily attainable with SPECT/CT, using the CT data for attenuation correction, thereby allowing more precise quantification of regional ventilation and perfusion. This approach has been used to improve the quantification of lobar perfusion prior to surgery [75]. In addition, quantitative ventilation/perfusion SPECT/CT is now being explored to guide radiation treatment planning, improving the ability to avoid delivering unnecessary radiation dose to higher functioning lung units (Fig. 4). Thus, the availability of SPECT/CT should encourage further study geared at improving the current clinical practice of assessing lung ventilation and perfusion.

Future directions

Molecular imaging approaches promise to provide important information regarding cellular activity and function that can be combined with anatomical information from other modalities to better characterize both lung parenchymal disease and lung cancers. In addition, newer molecular-based technologies relying on optical or ultrasonic emissions, using either inherent tissue properties or exogenously administered dyes [76–78], could further expand the scope of multimodality imaging in the lungs. If bronchoscopes with sensors adapted for such optical and ultrasonic imaging were developed, it is possible to imagine that the imaging information obtained from PET, SPECT, CT, and MR could be used to guide the bronchoscopic evaluation, or that the local information obtained

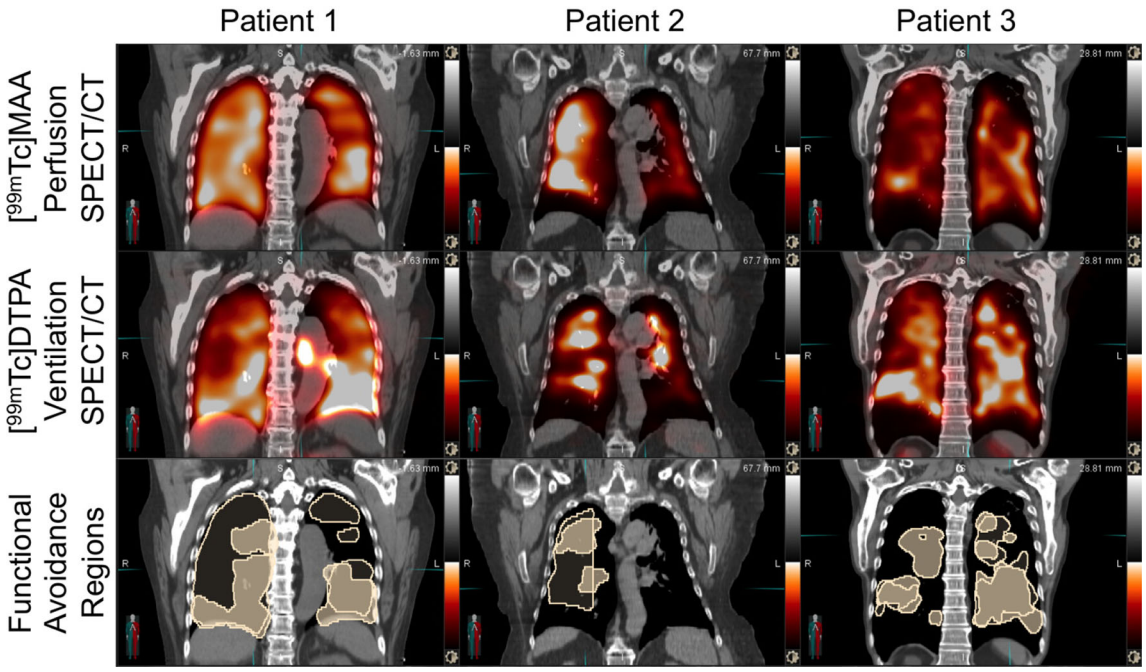

Fig. 4 SPECT/CT imaging of perfusion and ventilation for functional lung definition. *Top* three patients display non-uniform uptake of 99mTc-MAA lung perfusion. *Middle* 99mTc-DTPA lung ventilation. *Bottom* avoidance regions were defined by a gradient search algorithm and show variable overlap between high perfusion (*transparent contour*) and high ventilation (*opaque contour*). Courtesy of Steven Bowen and Jing Zeng, Departments of Radiology and Radiation Oncology, University of Washington (color figure online)

by bronchoscopy could be used to validate a signature that could be assessed throughout the entire lungs by means of whole-body scanners. Thus, multifunctional probes that are labeled for PET and acoustic or optical imaging would further enable such combined bronchoscopy-imaging investigations [79]. Even combined PET/MR probes could leverage the strengths of each modality to obtain more detailed molecular imaging signatures of lung disease.

Conclusion

In summary, the technical advances enabling simultaneous PET/MR acquisitions, in addition to further refinements in PET/CT and SPECT/CT acquisitions, have created opportunities to better investigate, through imaging, the relationships between molecular activity, lung function and anatomy. Further study using these imaging approaches in patients will best determine the full potential of these technologies to advance patient care and ultimately improve outcomes of lung disease treatment.

Acknowledgments This work was supported in part by NIH grants R01CA160253, U01-CA148131, R01HL116389, R01HL121218, and a Clinical Investigator Award from the Doris Duke Charitable Foundation to D. Chen.

Conflict of interest Neither Delphine L. Chen nor Paul E. Kinahan have any conflicts of interest to declare.

Human and animal studies This article does not contain any studies with human or animal subjects performed by any of the authors.

References

1. National Heart Lung Blood Institute (2012) Morbidity and Mortality: 2012 Chart Book on Cardiovascular, lung, and blood diseases. https://www.nhlbi.nih.gov/files/docs/research/2012_ChartBook.pdf. Accessed 26 Sept 2014
2. Mathers CD, Loncar D (2006) Projections of global mortality and burden of disease from 2002 to 2030. PLoS Med 3:e442
3. American Cancer Society (2014) Cancer facts and figures 2014. http://www.cancer.org/acs/groups/content/@research/documents/webcontent/acspc-042151.pdf. Accessed 26 Sept 2014
4. Martinez FJ, Donohue JF, Rennard SI (2011) The future of chronic obstructive pulmonary disease treatment—difficulties of and barriers to drug development. Lancet 37:1027–1037
5. Cherry SR, Sorenson JA, Phelps ME (2012) Physics in nuclear medicine, 4th edn. Saunders, Philadelphia
6. Huang SC (2000) Anatomy of SUV. Standardized uptake value. Nucl Med Biol 27:643–646
7. Thie JA (2004) Understanding the standardized uptake value, its methods, and implications for usage. J Nucl Med 45:1431–1434
8. Boellaard R (2009) Standards for PET image acquisition and quantitative data analysis. J Nucl Med 50:11S–120S
9. Kinahan PE, Doot RK, Wanner-Roybal M et al (2009) PET/CT assessment of response to therapy: tumor change measurement, truth data, and error. Transl Oncol 2:223–230
10. Lederlin M, Crémillieux Y (2014) Three-dimensional assessment of lung tissue density using a clinical ultrashort echo time at 3 tesla: a feasibility study in healthy subjects. J Magn Reson Imaging 40:839–847

11. Ma W, Sheikh K, Svenningsen S et al (2014) Ultra-short echo-time pulmonary MRI: evaluation and reproducibility in COPD subjects with and without bronchiectasis. J Magn Reson Imaging. doi:10.1002/jmri.24680
12. McCollough CH, Christner JA, Kofler JM (2010) How effective is effective dose as a predictor of radiation risk? AJR Am J Roentgenol 194:890–896
13. Yamashiro T, Miyara T, Honda O et al (2014) Adaptive iterative dose reduction using three dimensional processing (AIDR3D) improves chest CT image quality and reduces radiation exposure. PLoS One 9:e105735
14. Yamada Y, Jinzaki M, Hosokawa T et al (2012) Dose reduction in chest CT: comparison of the adaptive iterative dose reduction 3D, adaptive iterative dose reduction, and filtered back projection reconstruction techniques. Eur J Radiol 81:4185–4195
15. Khawaja RD, Singh S, Lira D et al (2014) Role of compressive sensing technique in dose reduction for chest computed tomography: a prospective blinded clinical study. J Comput Assist Tomogr 38:760–767
16. Ernst CW, Basten IA, Ilsen B et al (2014) Pulmonary disease in cystic fibrosis: assessment with chest CT at chest radiography dose levels. Radiology 25:132–201
17. Medicine AAOPI AAPM Position Statement on Radiation Risks from Medical Imaging Procedures. Policy Number PP 25-A, Policy date 12/13/2011, Sunset date 12/31/2016 https://www.aapm.org/org/policies/details.asp?id=318&type=PP&current=true
18. Chen DL, Mintun MA, Schuster DP (2004) Comparison of methods to quantitate ^{18}F-FDG uptake with PET during experimental acute lung injury. J Nucl Med 45:1583–1590
19. Kinahan PE, Fletcher JW (2010) Positron emission tomography-computed tomography standardized uptake values in clinical practice and assessing response to therapy. Semin Ultrasound CT MR 31:496–505
20. Disselhorst JA, Bezrukov I, Kolb A, Parl C, Pichler BJ (2014) Principles of PET/MR imaging. J Nucl Med 55:2S–10S
21. Doot RK, Pierce LA, Byrd D et al (2014) Biases in multicenter longitudinal PET standardized uptake value measurements. Transl Oncol 7:48–54
22. Quick HH (2014) Integrated PET/MR. J Magn Reson Imaging 39:243–258
23. Madsen MT (2007) Recent advances in SPECT imaging. J Nucl Med 48:661–673
24. Celler A, Farncombe T, Bever C et al (2000) Performance of the dynamic single photon emission computed tomography (dSPECT) method for decreasing or increasing activity changes. Phys Med Biol 45:3525–3543
25. Hasegawa BH, Iwata K, Wong KH et al (2002) Dual-modality imaging of function and physiology. Acad Radiol 9:1305–1321
26. Kinahan PE, Hasegawa BH, Beyer T (2003) X-ray based attenuation correction for positron emission tomography/computed tomography scanners. Semin Nucl Med 33:166–179
27. Kinahan PE, Townsend DW, Beyer T, Sashin D (1998) Attenuation correction for a combined 3D PET/CT scanner. Med Phys 25:2046–2253
28. Zhi-Pei L, Lauterbur PC (1999) Principles of magnetic resonance imaging: a signal processing perspective. Wiley, New York
29. Lutterbey G, Gieseke J, von Falkenhausen M, Morakkabati N, Schild H (2005) Lung MRI at 3.0 T: a comparison of helical CT and high-field MRI in the detection of diffuse lung disease. Eur Radiol 15:324–328
30. Martinez-Moller A, Souvatzoglou M, Delso G et al (2009) Tissue classification as a potential approach for attenuation correction in whole-body PET/MRI: evaluation with PET/CT data. J Nucl Med 50:520–526
31. Gilman MD, Fischman AJ, Krishnasetty V, Halpern EF, Aquino SL (2006) Optimal CT breathing protocol for combined thoracic PET/CT. Am J Roentgenol 187:1357–1360
32. Goerres GW, Kamel E, Heidelberg TN et al (2002) PET-CT image co-registration in the thorax: influence of respiration. Eur J Nucl Med Mol Imaging 29:351–360
33. Kawano T, Ohtake E, Inoue T (2008) Deep-inspiration breath-hold PET/CT of lung cancer: maximum standardized uptake value analysis of 108 patients. J Nucl Med 49:1223–1231
34. Liu C, Pierce LA 2nd, Alessio AM, Kinahan PE (2009) The impact of respiratory motion on tumor quantification and delineation in static PET/CT imaging. Phys Med Biol 54:7345–7362
35. Boucher L, Rodrigue S, Lecomte R, Benard F (2004) Respiratory gating for 3-dimensional PET of the thorax: feasibility and initial results. J Nucl Med 45:214–219
36. Chi PC, Mawlawi O, Luo D et al (2008) Effects of respiration-averaged computed tomography on positron emission tomography/computed tomography quantification and its potential impact on gross tumor volume delineation. Int J Radiat Oncol Biol Phys 71:890–899
37. Nehmeh SA, Erdi YE, Pan T et al (2004) Four-dimensional (4D) PET/CT imaging of the thorax. Med Phys 31:3179–3186
38. Kinahan PE, MacDonald L, Ng L, et al. (2006) Compensating for patient respiration in PET/CT imaging with the registered and summed phases (RASP) procedure. 3rd IEEE International Symposium on Biomedical Imaging: Nano to Macro. 1104–11107. http://ieeexplore.ieee.org/xpl/login.jsp?tp=&arnumber=1625115&url=http%3A%2F%2Fieeexplore.ieee.org%2Fxpls%2Fabs_all.jsp%3Farnumber%3D1625115
39. Nehmeh SA, Erdi YE (2008) Respiratory motion in positron emission tomography/computed tomography: a review. Semin Nucl Med 38:167–176
40. Wurslin C, Schmidt H, Martirosian P et al (2013) Respiratory motion correction in oncologic PET using T1-weighted MR imaging on a simultaneous whole-body PET/MR system. J Nucl Med 54:464–471
41. Paul NS, Ley S, Metser U (2012) Optimal imaging protocols for lung cancer staging: CT, PET, MR imaging, and the role of imaging. Radiol Clin North Am 50:935–949
42. Weber WA, Grosu AL, Czernin J (2008) Technology Insight: advances in molecular imaging and an appraisal of PET/CT scanning. Nat Clin Pract Oncol 5:160–170
43. Drzezga A, Souvatzoglou M, Eiber M et al (2012) First clinical experience with integrated whole-body PET/MR: comparison to PET/CT in patients with oncologic diagnoses. J Nucl Med 53:845–855
44. Schmidt H, Brendle C, Schraml C et al (2013) Correlation of simultaneously acquired diffusion-weighted imaging and 2-deoxy-[^{18}F] fluoro-2-D-glucose positron emission tomography of pulmonary lesions in a dedicated whole-body magnetic resonance/positron emission tomography system. Invest Radiol 48:247–255
45. Souvatzoglou M, Eiber M, Takei T et al (2013) Comparison of integrated whole-body [^{11}C]choline PET/MR with PET/CT in patients with prostate cancer. Eur J Nucl Med Mol Imaging 40:1486–1499
46. Al-Nabhani KZ, Syed R, Michopoulou S et al (2014) Qualitative and quantitative comparison of PET/CT and PET/MR imaging in clinical practice. J Nucl Med 55:88–94
47. Pace L, Nicolai E, Luongo A et al (2014) Comparison of whole-body PET/CT and PET/MRI in breast cancer patients: lesion detection and quantitation of ^{18}F-deoxyglucose uptake in lesions and in normal organ tissues. Eur J Radiol 83:289–296
48. Kershah S, Partovi S, Traughber BJ et al (2013) Comparison of standardized uptake values in normal structures between PET/CT

and PET/MRI in an oncology patient population. Mol Imaging Biol 15:776–785
49. Ohno Y, Koyama H, Onishi Y et al (2008) Non-small cell lung cancer: whole-body MR examination for M-stage assessment–utility for whole-body diffusion-weighted imaging compared with integrated FDG PET/CT. Radiology 248:643–654
50. Plathow C, Aschoff P, Lichy MP et al (2008) Positron emission tomography/computed tomography and whole-body magnetic resonance imaging in staging of advanced nonsmall cell lung cancer–initial results. Invest Radiol 43:290–297
51. Yi CA, Shin KM, Lee KS et al (2008) Non-small cell lung cancer staging: efficacy comparison of integrated PET/CT versus 3.0-T whole-body MR imaging. Radiology 248:632–642
52. Heusch P, Buchbender C, Kohler J et al (2014) Thoracic staging in lung cancer: prospective comparison of ^{18}F-FDG PET/MR imaging and ^{18}F-FDG PET/CT. J Nucl Med 55:373–378
53. Wang LL, Lin J, Liu K et al (2014) Intravoxel incoherent motion diffusion-weighted MR imaging in differentiation of lung cancer from obstructive lung consolidation: comparison and correlation with pharmacokinetic analysis from dynamic contrast-enhanced MR imaging. Eur Radiol 24:1914–1922
54. Weber WA, Czernin J, Phelps ME, Herschman HR (2008) Technology Insight: novel imaging of molecular targets is an emerging area crucial to the development of targeted drugs. Nat Clin Pract Oncol 5:44–54
55. Kahraman D, Holstein A, Scheffler M et al (2012) Tumor lesion glycolysis and tumor lesion proliferation for response prediction and prognostic differentiation in patients with advanced non-small cell lung cancer treated with erlotinib. Clin Nucl Med 37:1058–1064
56. Zander T, Scheffler M, Nogova L et al (2011) Early prediction of nonprogression in advanced non-small-cell lung cancer treated with erlotinib by using [(^{18})F]fluorodeoxyglucose and [(^{18})F]fluorothymidine positron emission tomography. J Clin Oncol 29:1701–1708
57. Mileshkin L, Hicks RJ, Hughes BG et al (2011) Changes in ^{18}F-fluorodeoxyglucose and ^{18}F-fluorodeoxythymidine positron emission tomography imaging in patients with non-small cell lung cancer treated with erlotinib. Clin Cancer Res 17:3304–3315
58. Yamamoto S, Korn RL, Oklu R (2014) ALK Molecular phenotype in non-small cell lung cancer: CT radiogenomic characterization. Radiology 272:568–576
59. Nair VS, Gevaert O, Davidzon G et al (2012) Prognostic PET ^{18}F-FDG uptake imaging features are associated with major oncogenomic alterations in patients with resected non-small cell lung cancer. Cancer Res 72:3725–3734
60. Rodrigues G, Lock M, D'Souza D, Yu E, Van Dyk J (2004) Prediction of radiation pneumonitis by dose-volume histogram parameters in lung cancer—a systematic review. Radiother Oncol 71:127–138
61. Hart JP, McCurdy MR, Ezhil M et al (2008) Radiation pneumonitis: correlation of toxicity with pulmonary metabolic radiation response. Int J Radiat Oncol Biol Phys 71:967–971
62. MacManus MP, Ding Z, Hogg A et al (2011) Association between pulmonary uptake of fluorodeoxyglucose detected by positron emission tomography scanning after radiation therapy for non-small-cell lung cancer and radiation pneumonitis. Int J Radiat Oncol Biol Phys 80:1365–1371
63. Petit SF, van Elmpt WJ, Oberije CJ et al (2011) [^{18}F]fluorodeoxyglucose uptake patterns in lung before radiotherapy identify areas more susceptible to radiation-induced lung toxicity in non-small-cell lung cancer patients. Int J Radiat Oncol Biol Phys 81:698–705
64. Elizur A, Cannon CL, Ferkol TW (2008) Airway inflammation in cystic fibrosis. Chest 133:489–495
65. McDonough JE, Yuan R, Suzuki M et al (2011) Small-airway obstruction and emphysema in chronic obstructive pulmonary disease. N Engl J Med 365:1567–1575
66. Jones HA, Marino PS, Shakur BH, Morrell NW (2003) In vivo assessment of lung inflammatory cell activity in patients with COPD and asthma. Eur Respir J 21:567–573
67. Subramanian R, Jenkins DL (2011) The evaluation and control of lung inflammation assessed with PET scanning in emphysema alpha-1 antitrypsin deficiency (Eclipse-AATD) Trial. Am J Respir Crit Care Med 183:A6152
68. Torigian DA, Dam V, Chen X et al (2013) In vivo quantification of pulmonary inflammation in relation to emphysema severity via partial volume corrected ^{18}F-FDG-PET using computer-assisted analysis of diagnostic chest CT. Hell J Nucl Med 16:12–18
69. Klein M, Cohen-Cymberknoh M, Armoni S et al (2009) ^{18}F-fluorodeoxyglucose-PET/CT imaging of lungs in patients with cystic fibrosis. Chest 136:1220–1228
70. Amin R, Charron M, Grinblat L et al (2012) Cystic fibrosis: detecting changes in airway inflammation with FDG PET/CT. Radiology 264:868–875
71. Wielputz MO, Puderbach M, Kopp-Schneider A et al (2014) Magnetic resonance imaging detects changes in structure and perfusion, and response to therapy in early cystic fibrosis lung disease. Am J Respir Crit Care Med 189:956–965
72. Kirby M, Pike D, Coxson HO et al (2014) Hyperpolarized 3He ventilation defects used to predict pulmonary exacerbations in mild to moderate chronic obstructive pulmonary disease. Radiology 24:140161
73. Miller GW, Mugler JP 3rd, Sá RC et al (2014) Advances in functional and structural imaging of the human lung using proton MRI. NMR Biomed. doi:10.1002/nbm.3156
74. Leblanc M, Paul N (2010) V/Q SPECT and computed tomographic pulmonary angiography. Semin Nucl Med 40:426–441
75. Toney LK, Wanner M, Miyaoka RS et al (2014) Improved prediction of lobar perfusion contribution using technetium-99 m-labeled macroaggregate of albumin single photon emission computed tomography/computed tomography with attenuation correction. J Thorac Cardiovasc Surg. doi:10.1016/j.jtcvs.2014.04.036
76. An f, Deng Z, Ye J, et al. (2014) Aggregation-induced near-Infrared (NIR) absorption of squaraine dye in an albumin nanocomplex for photoacoustic tomography in vivo. ACS Appl Mater Interfaces [Epub ahead of print]
77. Hou R, Le T, Murgu SD, Chen Z, Brenner M (2011) Recent advances in optical coherence tomography for the diagnoses of lung disorders. Expert Rev Respir Med 5:711–724
78. Zhang HF, Maslov K, Stoica G, Wang LV (2006) Functional photoacoustic microscopy for high-resolution and noninvasive in vivo imaging. Nat Biotechnol 24:848–851
79. Lewis MR, Kannan R (2014) Development and applications of radioactive nanoparticles for imaging of biological systems. Wiley Interdiscip Rev Nanomed Nanobiotechnol. doi:10.1002/wnan.1292